Available online at www.sciencedirect.com
SCIENCE DIRECT®
International Journal of Heat and Mass Transfer 48 (2005) 5371–5385
International Journal of HEAT and MASS TRANSFER
www.elsevier.com/locate/ijhmt

Visualization of a principle mechanism of critical heat flux in pool boiling

In Cheol Bang [a,*], Soon Heung Chang [a], Won-Pil Baek [b]

[a] Korea Advanced Institute of Science and Technology, 373-1, Guseong-dong, Yuseong-gu, Daejeon 305-701, Republic of Korea
[b] Korea Atomic Energy Research Institute, 150, Dukjin-dong, Yuseong-gu, Daejeon 305-353, Republic of Korea

Received 2 February 2005; received in revised form 1 July 2005
Available online 2 September 2005

Abstract

A new experimental work was made to discover a principle mechanism of the burnout in pool boiling. Here, we directly observed a liquid layer structure under a massive vapor clot and the liquid layer-related burnout phenomenon. Based on the present observations, we have made a visual model for the formation and dryout of a liquid film under its vapor environment. At the formation process, liquid is trapped in interleaved space between growing bubbles and surface and the liquid trapping continues between coalesced bubbles and surface. In the dryout process, we especially observed vapor "holes" made by spontaneous breakup of discrete nucleating bubbles inside a vapor clot. The burnout can be triggered by the evaporation of the liquid film region expanded from rims of the holes.

Keywords: Liquid film; Macrolayer; Critical heat flux; Boiling; Visualization

1. Introduction

When a liquid coolant undergo a change in phase absorbing heat from a heated solid surface, higher heat transfer rates is taken advantage of. The more efficient heat transfer results from the removal of heat from the heated surface as heat of vaporization and sensible heat and the motions of the bubbles leading to rapid mixing of the fluid. Therefore, boiling heat transfer has played an important role in industrial heat transfer processes [1] such as macroscopic heat transfer exchangers in nuclear and fossil power plants, and microscopic heat transfer devices of heat pipes and microchannels for cooling electronic chips. Moreover, the core technology that made a commercial success of thermal ink-jet printers is based on the application of boiling bubbles, which propel tiny ink droplets through the openings of an ink cartridge [2,18]. The use of boiling is limited by critical heat flux (CHF) which is also called as boiling crisis or departure from nucleate boiling. The most serious problem is that the boiling limitation can be directly related to the physical burnout of the materials of a heated surface due to comparatively inefficient heat transfer through a vapor film formed across the surface. Therefore, CHF is the most important factor of information required for the design of a system with heat transferred or generated. In spite of last half century of so many intensive and extensive efforts, however, the physical mechanism triggering this limitation has not been

* Corresponding author. Tel.: +82 42 869 3856; fax: +82 42 869 3810.
E-mail address: musoyou@kaist.ac.kr (I.C. Bang).

0017-9310/$ - see front matter © 2005 Elsevier Ltd. All rights reserved.
doi:10.1016/j.ijheatmasstransfer.2005.07.006

Nomenclature

A	heated area or heated area covered by vapor
g	gravity
h	latent heat or heat transfer coefficient
q	heat flux
t	time
T	temperature

Greek symbols

δ	macrolayer thickness
ρ	density of liquid

Subscripts

f	bulk liquid or saturated liquid
fg	latent heat of vaporization
h	hovering time
w	heated surface
v	vapor

understood clearly [3]. What is the real mechanism triggering the limitation? To explain the mechanism behind the boiling limitation, there are two classical hypotheses [4]: one hypothesis considers the obstructions of heat transfer due to vapor masses anchored on the heated surface, and the other hypothesis postulates that the limitation is due to the existence of a limit in the state of the fluid system; for example, there are geometrical theories based on critical bubble spacing near the heated surface and hydrodynamic ones based on the instability of the interface between liquid and vapor.

However, visual observations have not confirmed either hypothesis. There are different interpretations for even a same observation. For this, Bergles [17] says that usually, one sees what one wants to see to support a particular mechanistic model or hypothesis. Fortunately, in relation to the mechanisms, there is a general consensus that fully developed nucleate boiling on a heated surface is characterized by the existence of a liquid film on the heated surface [3]. The occurrence of the boiling limitation has been linked closely to the behavior of the liquid film. This liquid film is generally referred to as the "thin liquid layer" or the "macrolayer" to distinguish it from the microlayer that exists under the base of discrete nucleating bubbles [3]. The question to be answered is whether a stable thin liquid layer under a vapor boiling environment could actually exist. If so, what precisely is the role of such a liquid film in relation to the boiling limitation? Reliable answers will depend on direct experimental observations.

Currently, there has been no direct observation of the liquid layer. For example, the investigations of Gaertner and Westwater [5] and Kirby and Westwater [6] have supplied only indirect indications of the existence of such a liquid layer. Numerous subsequent studies have failed to provide a direct confirmation of a stable thin liquid layer under a vapor boiling environment. In 1977, Yu and Mesler [7] offered a hypothesis of the existence of the layer, as illustrated in Fig. 1(a). Katto and Yokoya [4] demonstrated the importance of Yu and Mesler's hypothesis; they used it to show that it is possible to approach the very complex boiling limitation phenomenon with a relatively simple liquid layer evaporation mechanism, using a simple energy balance equation, such as

$$t_h q A_w = \rho_f h_{fg} \delta (A_w - A_v). \quad (1)$$

As a result, the Katto and Yokoya hypothesis came to be accepted during the last half century, though actual proof of the layer has continued to elude many investigators.

In particular, based on very hypothetical vapor stems resulting from Gaertner and Westwater's observation and Katto and Yokoya's analysis, Haramura and Katto [16] proposed a new hydrodynamic hypothesis that Helmholtz instability is imposed on the vapor–liquid interface of columnar vapor stems distributed in a liquid layer wetting a heated surface in order to predict the thickness of the liquid layer. However, unfortunately this hydrodynamic hypothesis for a very thin liquid layer stirred up a lot of disputes and even the disputes have been threatening the general consensus of the existence of the liquid layer under a massive vapor environment characterizing the CHF limit. Recently, due to poor visual evidences for the consensus, some researchers are showing up while insisting that CHF limitation is closely linked to not a liquid film without direct observation but rather boiling activity and dry spots originating from nucleate boiling phenomena [10,11]. To say again, the reason of the mistrust is that there is no direct observation of the liquid layer.

The present work proposes a new method to surely prove the existence of the layer. Our method involves two new ideas. The first idea is that a direct observation of the layer can be achieved under an environment in which the liquid phase is distinguished clearly from the vapor phase. We use a nanofluid as a colored fluid in order to distinguish between the liquid phase and the vapor phase in a complex boiling environment. We

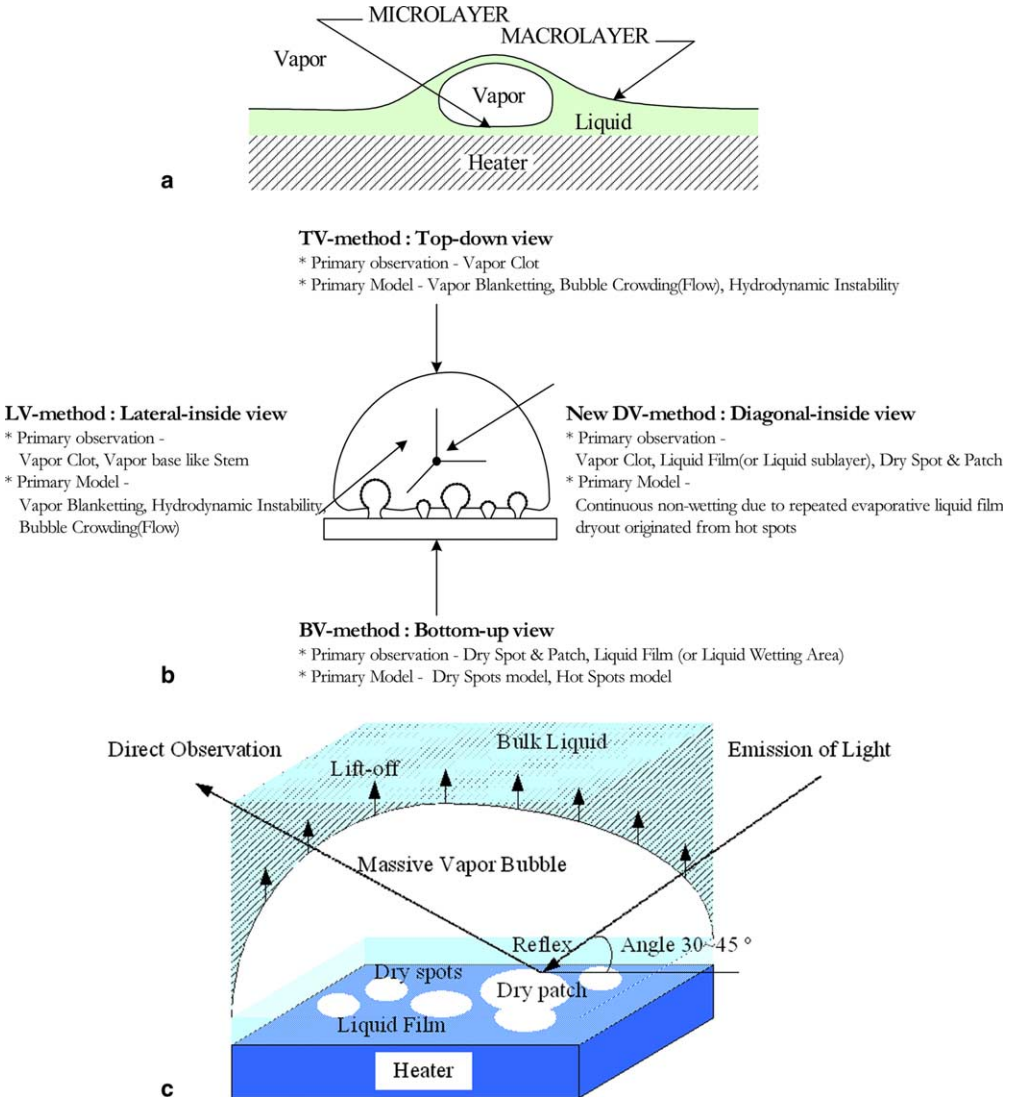

Fig. 1. Boiling structure and visualization: (a) conventional illustration of hypothesis for liquid film structure [7], (b) traditional and new approaches of visualization and their primary observations, (c) new ideas for the direct observation: a nanofluid as a dyed-water and diagonal–inside view for the observation.

chose alumina nanofluid with white color nanoparticles for this purpose. The fluids are prepared by dispersing alumina nanoparticles into water as a base fluid.

The second idea is that a direct observation of the layer can be achieved under a new view of visualization. Actually, we can intuitively divide the experimental observations and hypotheses into the three traditional groups of a top–down approach, a bottom–up approach, and a lateral–inside approach as shown in Fig. 1(b). One new diagonal–inside approach is newly introduced in the present work.

Fig. 1(c) shows the ideas: the white colored fluid and the new view of visualization. In this way, in the boiling, an internal structure under a massive vapor bubble can be displayed while the transparent vapor bubble lift off the white fluid with a driving force due to volume expansion.

With the method, observation and analysis of pool boiling at high heat fluxes are performed in the present study using high-speed photography and advanced digital photography. In order to make clear aims for visualization and its analysis, we specially summarized current issues [3,8–11] on the pool boiling CHF visualization as shown in Table 1, and then this paper will describe in turn on each issue.

Table 1
Current issues on visualization of pool boiling CHF

	Current issue [3,8–11]	Current status	Contribution	
			Expectation from traditional methods	Expectation from present DV-method
1	Active nucleation site density	△	○	△
2	Spatial distribution of active sites	○	○	△
3	Active site interaction	△	○ (BV-method)	△
4	Role of dry spot	×	○ (BV-method)	○
5	Dry area formation mechanism	×	○ (BV-method)	○
6	Existence of macrolayer	×	×	○
7	Macrolayer formation mechanism	×	×	○
8	Role of vapor stem	×	×	○
9	Thickness of macrolayer	×	×	△
10	Macrolayer dryout mechanism	×	×	○
11	Liquid resupply	×	×	○

×: Very disputing. △: Partially resolved. ○: Fully resolved.

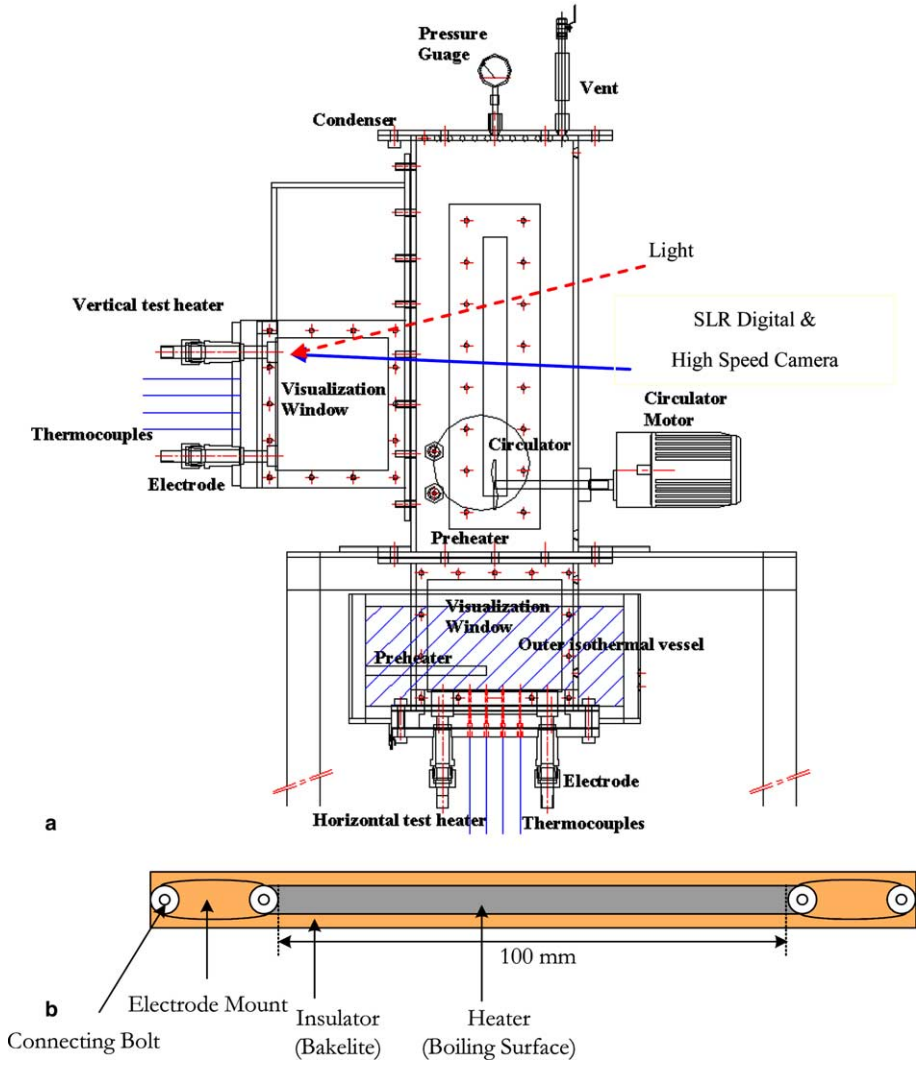

Fig. 2. Nanofluid boiling experimental facility: (a) pool boiling facility [13], (b) boiling surface geometry.

2. Experimental method

2.1. Pool boiling experimental facility

All tests for the direct observation were performed in pool boiling under atmospheric pressure. The pool boiling test facility is shown in Fig. 2(a). The facility consists of a main vessel, a horizontal test heater component with visualization windows, a vertical test heater component with visualization windows, an outer isothermal vessel, a pre-heater, a circulator, and a condenser. Pure water and nanofluids are filled in the main vessel.

A test plane heater with copper electrodes is heated by a DC power supply with a maximum capacity of 4.375 kW (5 V, 875 A). The boiling surface of the test plane heaters is $4 \times 100\ mm^2$ rectangular with a depth of 1.9 mm as shown in Fig. 2(b). At the back of the boiling surface, four holes are machined where 4K-type thermocouples are imbedded at a depth of 1 mm with silver welding to measure the boiling surface temperature. The surface roughness of the boiling surface is controlled by sandpaper of grade #2000. The signals of the thermocouples are acquired by a data acquisition system.

2.2. A dyed-water for a clear distinction between liquid and vapor

In this work, a dyed-water is prepared by dispersing alumina nanoparticles into water as a base fluid. The dyed-water with nanoparticles is originally called nanofluid. The fluid is generally used with stable, uniform and continuous suspension and without no outstanding chemical change of the base fluid and also physical properties of the alumina nanofluid are the most well known. Transmission electron microscopy (TEM) reveals alumina nanoparticles as having a spherical shape, with a normal size ranging from 15 nm to 124 nm (a 47 nm avg. diameter). In order to ensure stable, uniform, and continuous suspension, the dispersion solutions are vibrated in an ultrasonic bath for approximately 8 h immediately before a boiling test is performed [12,13]. Nanofluids generally in heat transfer area are used to increase heat transfer with high thermal conductivity

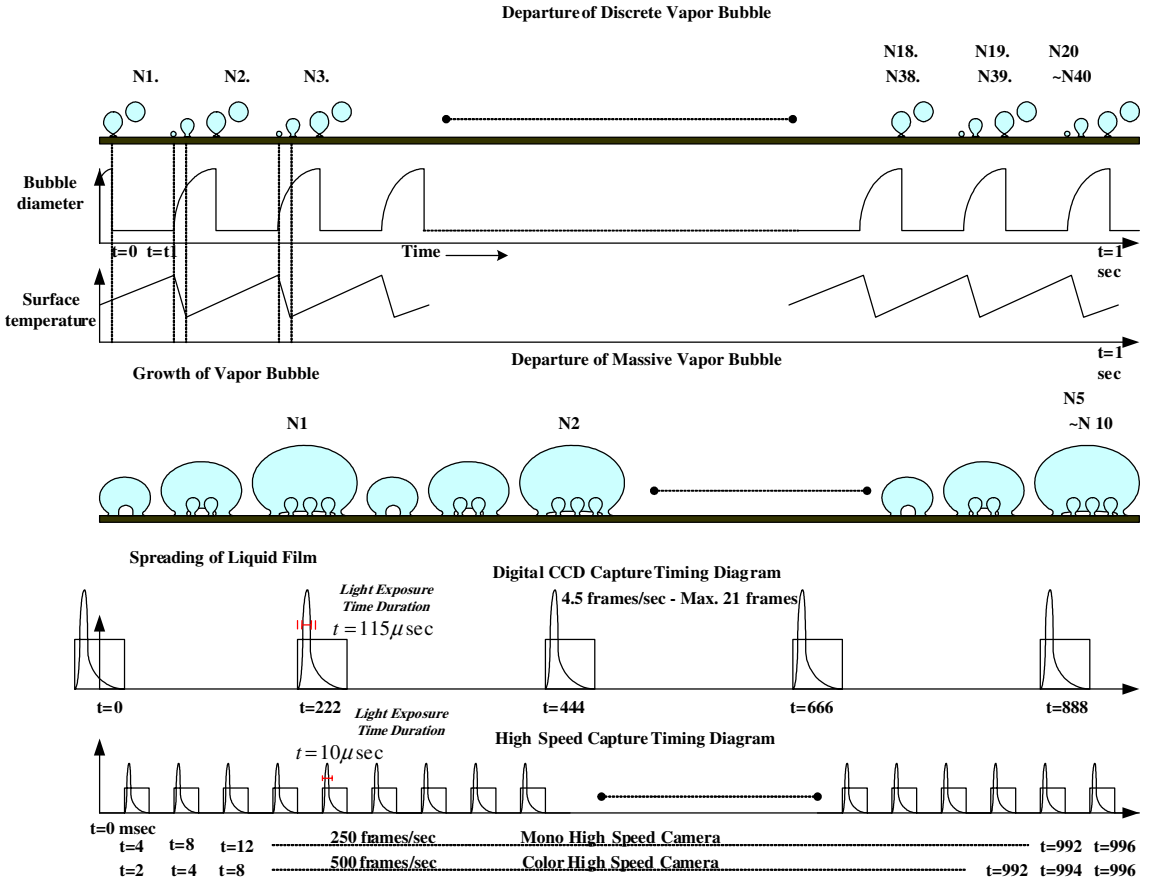

Fig. 3. Visualization capture timing for periodic boiling phenomena [14].

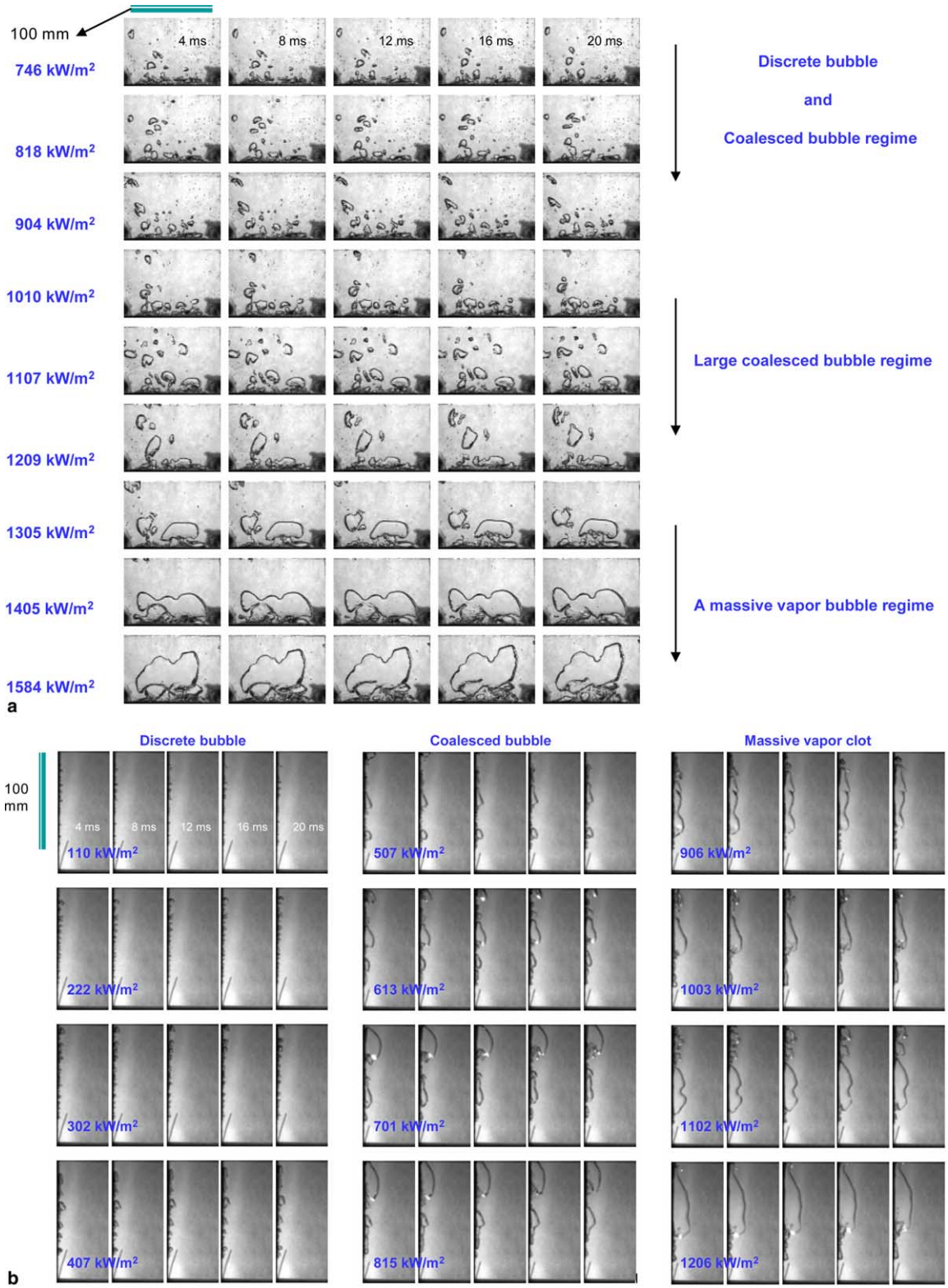

Fig. 4. Boiling phenomena for horizontal and vertical heated surfaces at pure water: (a) images of mono high-speed camera. 250 f/s, ~100 exp. μs, (b) images of mono high-speed camera. 250 f/s, ~100 exp. μs.

enhancement. Therefore, boiling heat transfer and critical heat flux values are also affected. In this paper, its effects will not be considered but those are reported in our previous nanofluid study [13]. Because boiling characteristics of nanofluids are similar to those of pure water such as bubble generation, coalescence and large vapor formation regardless of heat transfer enhancement mechanisms of the nanofluid [13], only we will focus on the phenomenon in each heat flux level expressed by a ratio of observational condition to critical heat flux.

2.3. Visualization technique

In this study, the boiling phenomena were visualized with an advanced digital photographic technique introduced in our previous visualization study [8,9] and a high-speed camera technique. The digital camera used has a flash-synchronized shutter speed of 1/500 s and a total 2.74 million pixels CCD. The optical lenses can be interchanged to increase magnification. As a light source, two flashes were used in single and double flash method that requires a synchronizing device.

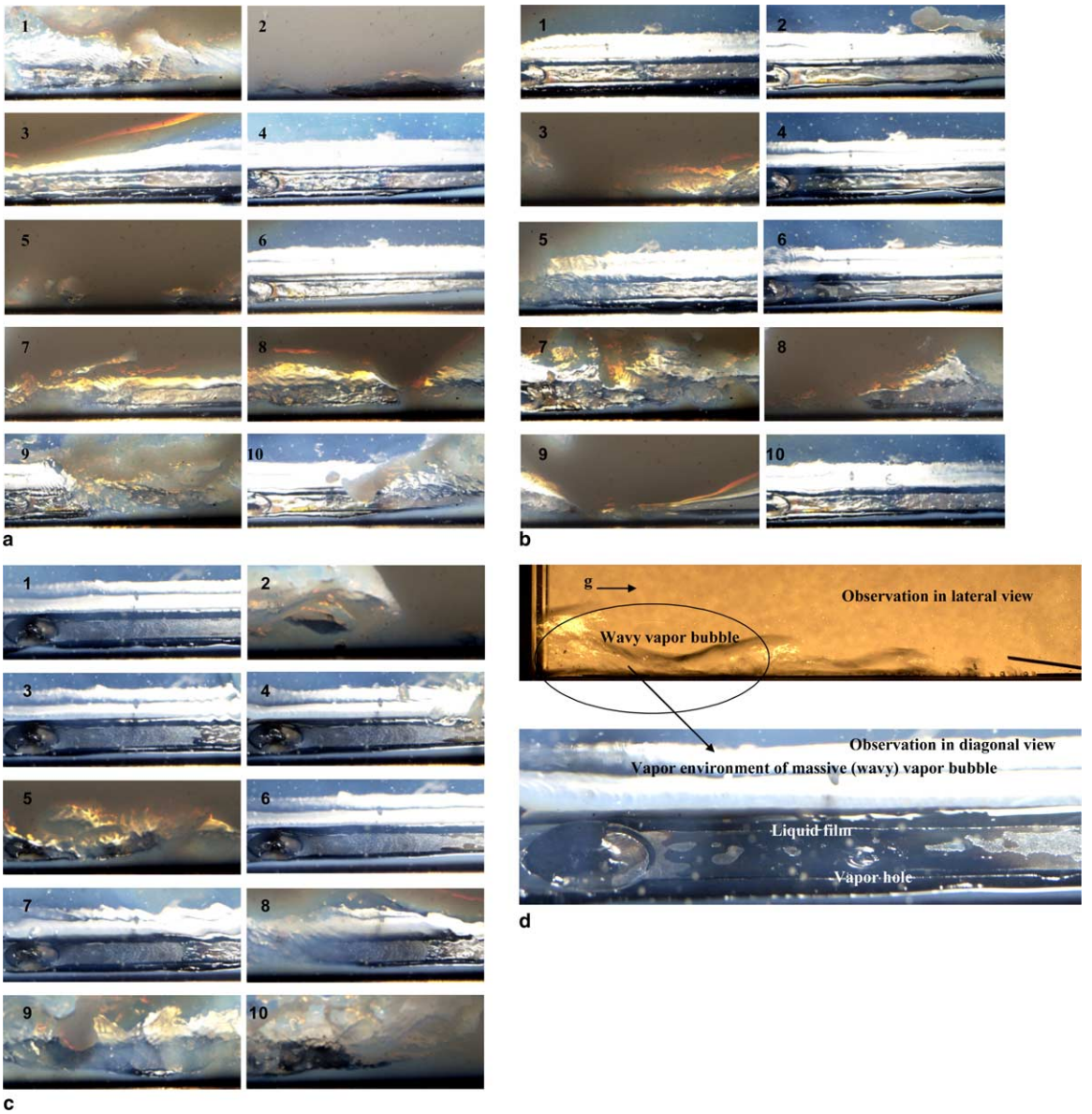

Fig. 5. Evidence of the liquid film: (a) 0.5 vol.% nanofluid, 90% CHF, (b) 0.5 vol.% nanofluid, 95% CHF, (c) 0.5 vol.% nanofluid, 100% CHF, (d) 0.5 vol.% nanofluid; 95% CHF.

Continuous photos were taken, with time interval of 0.22 s. To magnify the phenomena shown in the pool, a 105 mm Macrolens was used, along with three extension tubes of 14, 21, and 31 mm, for close–ups. After capturing the phenomena, image processing was performed, using commercial image processing software, to correct the brightness and contrast of the images. The digital camera provided a spatial resolution of ~10 μm per pixel to the images. In addition, as a high-speed capture system, mono camera and color camera with 10 μs time duration are used. With the visual systems, the visualization strategy as shown in Fig. 3 was adopted on boiling phenomena. As boiling is a periodical process of generation and departure of a bubble or a large vapor clot, a high-speed camera has a fast frame rate synchronized with very shot exposure time in order to observe an overall process. On the other hand, a digital camera could provide not a faster frame rate but much higher resolution in order to acquire a magnified image of the boiling process. Like this, the study properly used both cameras according to each advantage and bubble departure frequency.

3. Results and discussion

3.1. General boiling phenomena of water

Fig. 4 shows typical boiling phenomena through traditional observation of lateral view on horizontal and vertical flat heated surfaces at pure water. Apparently flow pattern is depending on a massive vapor clot formed by coalescences of bubbles with the increase of heat flux. This description has been well known through previously reported visual results due to same view of visualization. And so, in here, we could not find any new finding on the mechanisms of pool boiling and CHF. Therefore, we adopted the above-mentioned new method. However, we could apply the method to only vertical heated surface due to a geometrical restriction of the visualization test section. Our focus is to explore the inside of massive vapor clot using the method.

3.2. Direct observation of principle mechanism of CHF based on its issues

3.2.1. Macrolayer evidence

Our exploration for finding a liquid film under massive vapor clot gave such results as shown in Fig. 5. Images in Fig. 5 by a diagonal view show phenomena confirming the existence of a liquid film under a massive vapor bubble or vapor environment. Also, the images show a part (with ~60 mm length) of the direct Joule heating plate (heater) measured 4 mm (width) × 100 mm (length). In (d), a bubble just before spontaneous break-up is shown in the liquid film.

3.2.2. Macrolayer formation mechanism

Boiling and the boiling limitation are phenomena characterized by periodical processes or intermittent processes. In Fig. 6, a typical example of the generation process of a liquid film at a high heat flux level shows

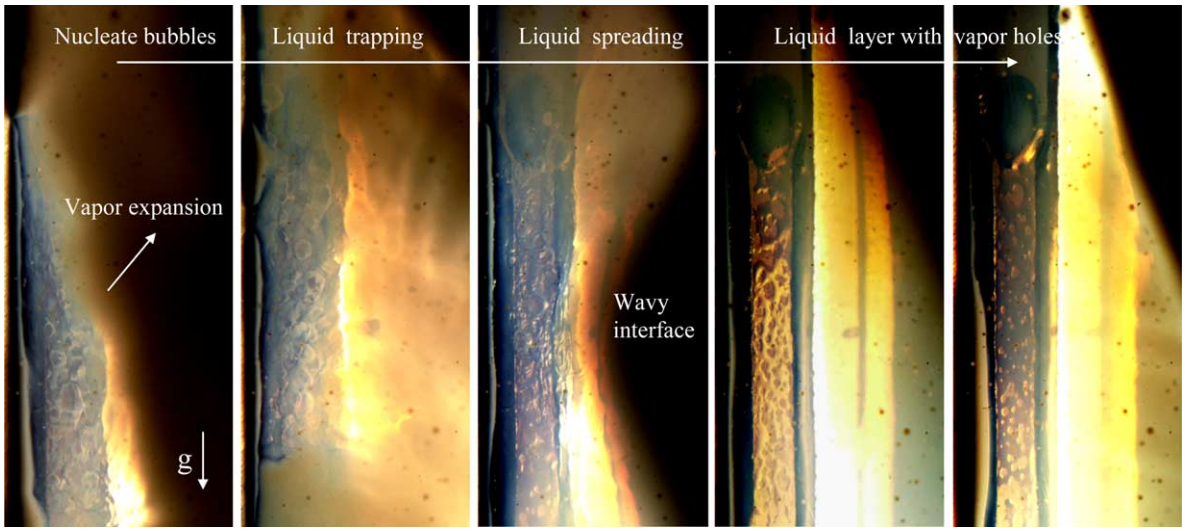

Fig. 6. Liquid film formation process: liquid trapped by nucleate bubbles in a expanding vapor environment from 4 vol.% Al_2O_3–water nanofluid at CHF is shown. Nucleate bubbles disappear little by little and a liquid region with small holes begins to appear. Liquid disturbed in the process spreads on the surface. The third image shows a typical wave interface by Taylor and Helmholtz instability theories.

that the generation proceeds through the formation of nucleate bubbles resulting in the growth of a massive vapor bubble. Liquid both internally trapped by means of both lateral and vertical coalescence of nucleate bubbles and externally supplied through triple phase line spreads on a solid surface while the bubbles form a massive vapor bubble due to the film itself consumption. In the other words, individual bubbles may lie above a thin liquid layer on a heater surface and the growth of the bubbles proceeds through the evaporation of the thin liquid. While spreading, some vapor holes are displayed inside the film as decreasing small holes. Vapor holes originate from the rupture of discrete individual nucleating bubbles. Later, the thin film is in a typical dryout stage, with evaporation in the rims of the vapor holes and in the overall liquid film-vapor interface. The film breaks up into local liquid fragments as shown in Fig. 7. Fig. 7(b) shows time evolution of dryout of the liquid film from 4 vol.% Al_2O_3–water nanofluid at CHF. The liquid spreading occurs after its trapping and the dryout process of a liquid film proceeds with its evaporation. In the top of an image, there is a non-heating part of the surface resulting in relative thicker interleaved liquid film without any dried area. In particular, the size of each vapor hole increases to contain a much larger dry area with evaporation around the rim in dryout process. Also, the vapor holes merge with neighboring holes, resulting in a large dry area. After a few msec, the surface is covered by only vapor or small liquid droplets, in place of the liquid.

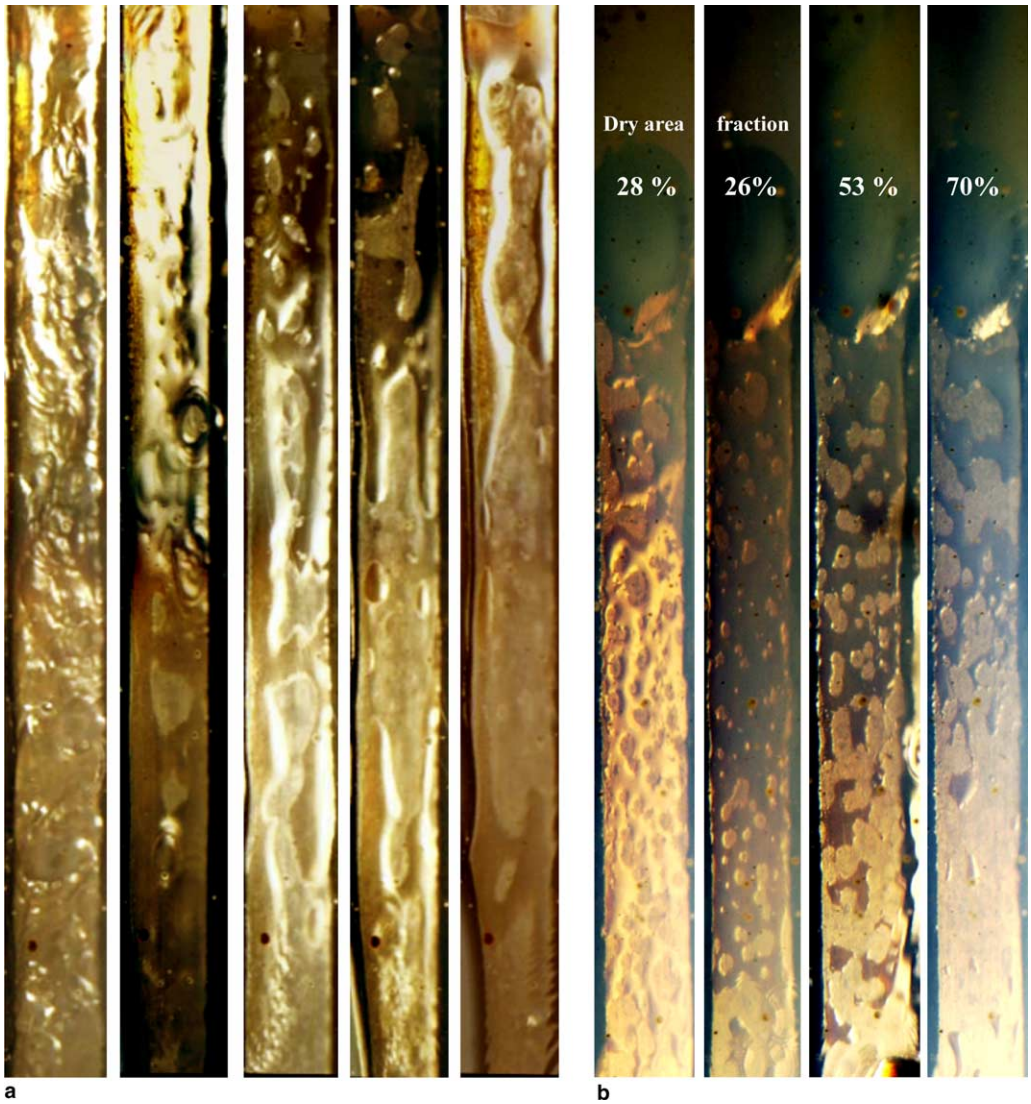

Fig. 7. Dynamic liquid film behavior at nanofluid: (a) 0.5 vol.% nanofluid, (b) 4 vol.% nanofluid.

3.2.3. Liquid resupply pathway

With a further increase in heat flux level, the liquid film dries out completely. Then, in accordance with the periodical process of boiling, a new liquid film forms, by means of the aforementioned trapping in the boiling, while the bulk liquid is again supplied near the surface and so the life and death of liquid film are repeated.

The intermittent resupply of liquid to the liquid film with the period of a massive vapor blanket is carried out apparently by the natural circulation according to boiling and fluid density as shown in Fig. 9(a). Actually, through the detailed observation of in Fig. 9(b), liquid could be also supplied by spreading from triple phase interface due to decrease of surface temperature by liquid film evaporation heat removal. In here, it is interesting that round areas like holes is covered by liquid finally. In addition, liquid drift due to a massive vapor bubble movement and natural circulation is surely shown in Fig. 9(c) visualized by diagonal–inside view.

3.2.4. Macrolayer dryout mechanism

Although liquid film dried out fully, the boiling limitation does not occur yet. Actually, at the boiling limitation, we can observe that the local part of the surface wetted by the liquid film does not rewet, as shown in Fig. 10. A limiting boundary between the non-wetting hot surface and the wetting cold surface is shown in a photo. Over time, the boundary expands to the wetting area with evaporation around the holes. The dryout of the part continues for much longer than for one of the periodical process. In contrast, in lower heat flux level apart from boiling limitation, a liquid film is sufficiently thick. Fig. 10(b) shows the time reconstruction of statistically representative dryout processes. The figure shows that the surface is not rewetted, which leads to burn-out of metal failure in boiling limitation.

Special attention should be given to the vapor holes in the liquid film. In Figs. 6–8, we present a typical hole–liquid structure. In the vapor environment, large vapor holes are seen inside the liquid film, whereas nucleate bubbles are seen just before the rupture for forming liquid film region, as shown in the lower part of the second image of Fig. 8(b). The liquid dries out with the expansion of the dried regions or the vapor holes due to evaporation from the rims of vapor holes. This resembles a dewetting process [15] which is characterized by holes and the motion of liquid rim apparently. The size and distribution of these vapor holes originally depends on the distribution of nucleation sites, whereas those of the observed vapor holes depend on the observation time in a period of the process. New illustration for vapor hole being formed by spontaneous breakup of a bubble is shown in Fig. 8(c).

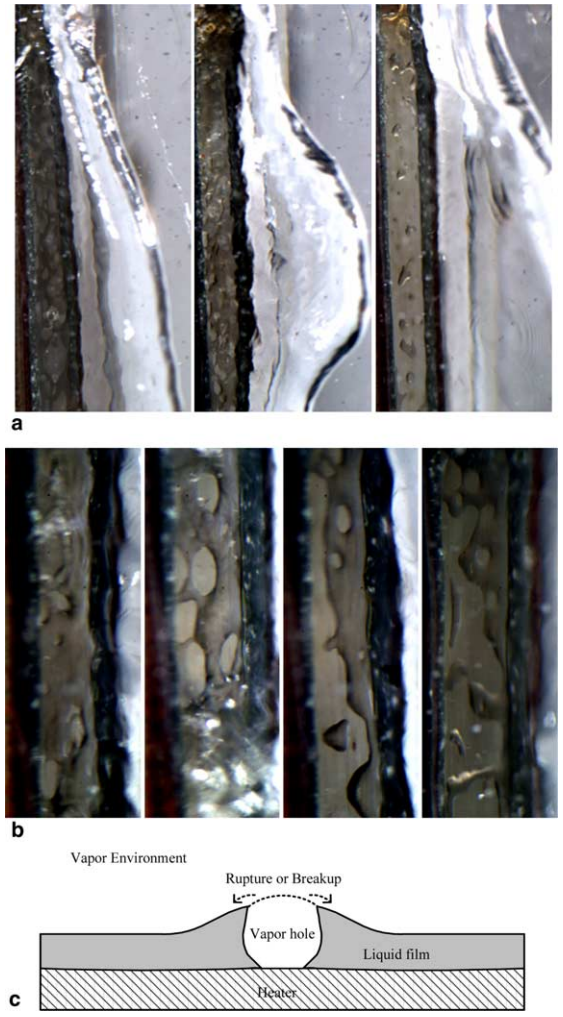

Fig. 8. Dynamic liquid film behavior at pure water and vapor hole: diagonal view method is tried in pure water. Although liquid layer is relatively less clear in pure water than in nanofluid, it is surely distinguished. (a) Vapor clot and liquid layer evaporation at pure water near CHF. (b) Magnification of the liquid film—vapor holes structure (85–100% CHF). (c) New illustration for vapor hole being formed by spontaneous breakup of a bubble.

3.2.5. Thickness of macrolayer

Several questions remain concerning the liquid film: How thick is the trapped liquid layer? What determines the thickness of the layer?

In this study, we could estimate the thickness with ~100 μm through the size of a nucleate bubble shown in thin liquid film of Fig. 5(d). The typical thickness of this layer is predicted to have a range from 50 to 500 μm for water on a flat horizontal surface, depending on the heat flux. There are many hypotheses regarding the factors that determine the thickness; such factors

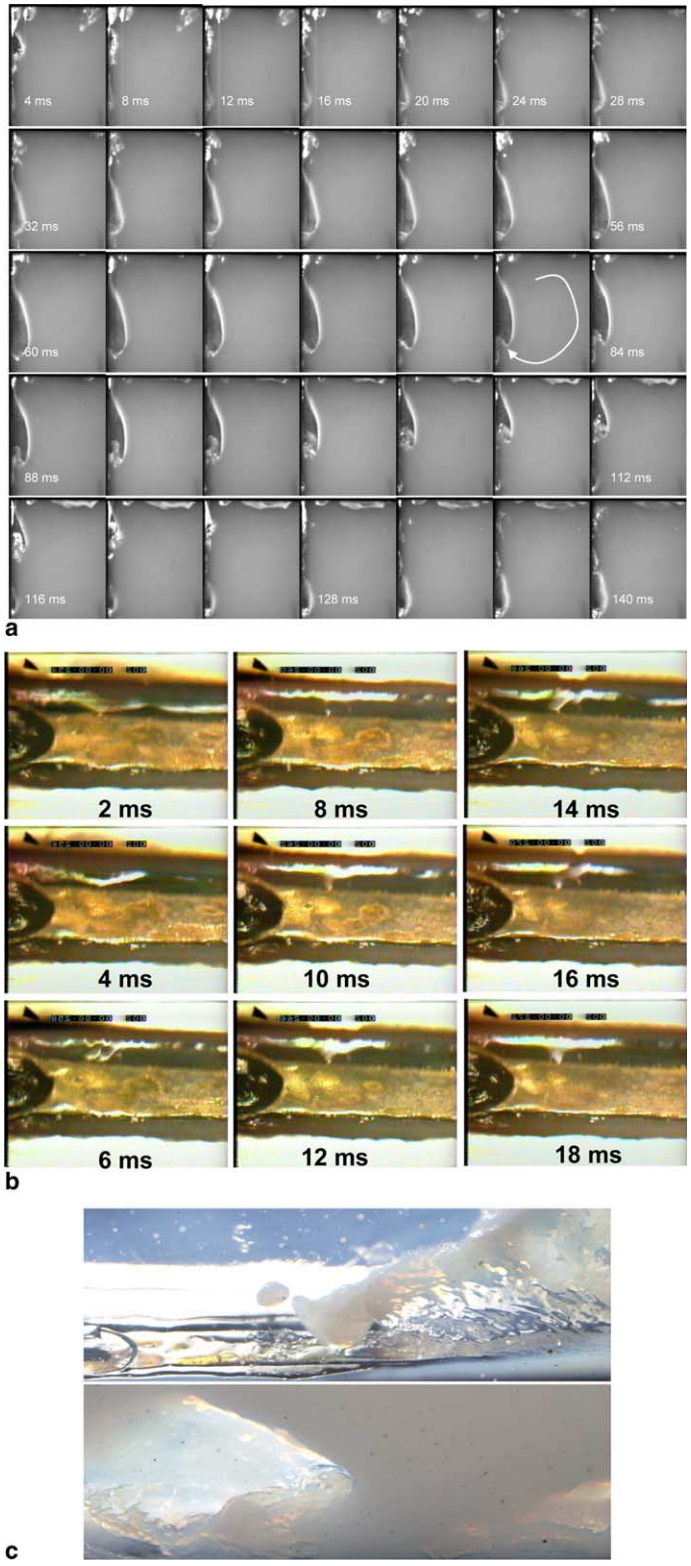

Fig. 9. Liquid resupply pathway: (a) life of a massive vapor bubble, (b) magnification of near-wall region: round areas to be covered by liquid finally and (c) liquid drift based on the liquid film into the vapor environment at 90% CHF.

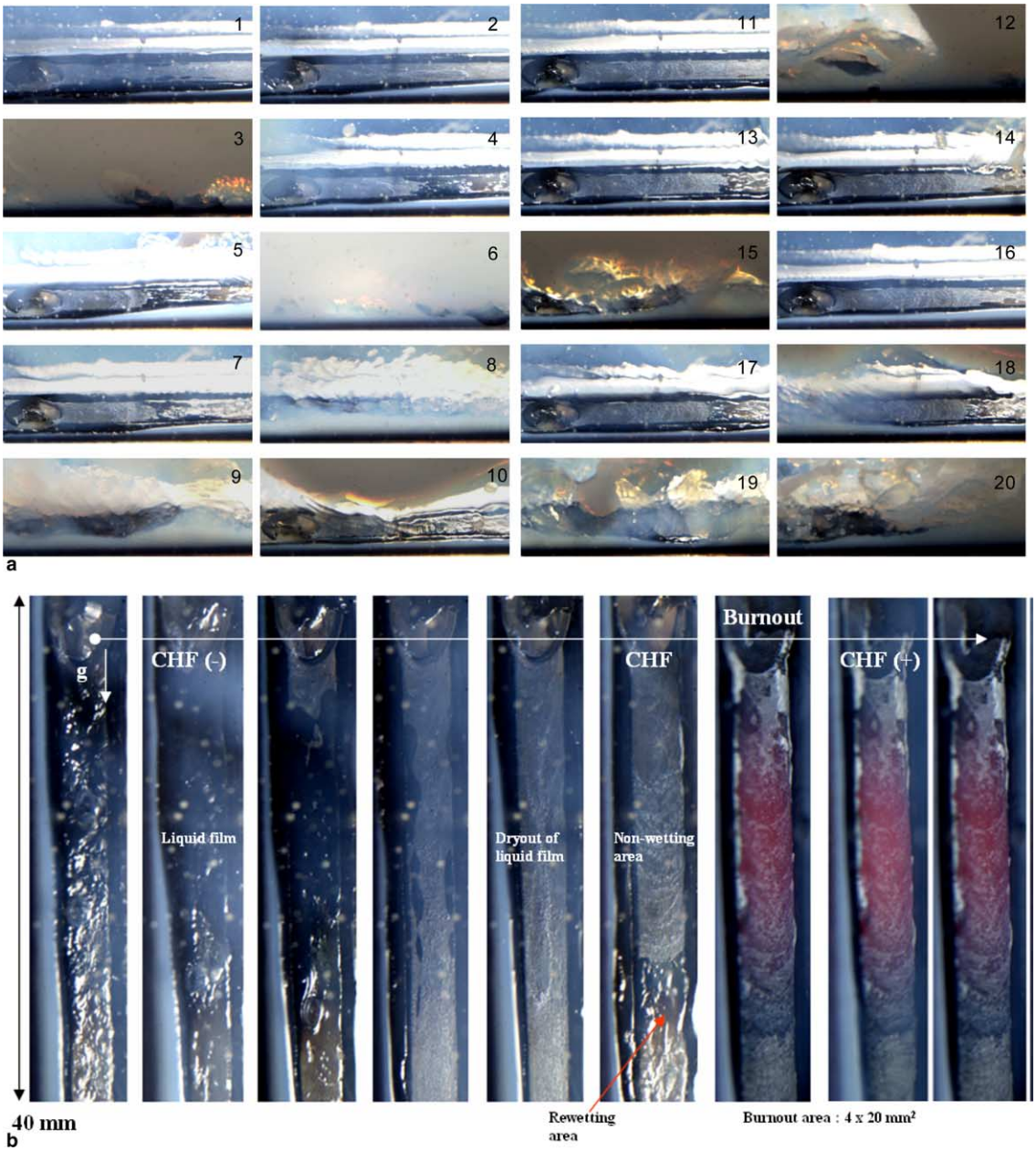

Fig. 10. Burn-out triggering mechanism: entirely dried and non-wettable surface of the heater glowed in CHF (+). (a) Appearance of non-wetting region: 0.5 vol.% nanofluid, ~100% CHF. (b) Burn-out phenomenon due to dryout of the liquid film.

could include Helmholtz instability, the contact angle, or the nucleation site density [3].

3.2.6. Burn-out triggering mechanism

Why does non-wetting of liquid in boiling limitation occur? The mechanism of the boiling limitation is that periodical wetting and dryout cause the rise of average temperature, and then the rise of average temperature prevents the wetting during the period of liquid resupply. Therefore, according to Newton's cooling law of

$$q = h(T_w - T_f), \tag{2}$$

the sudden falling of the heat transfer coefficient, due to the conversion of a liquid–solid interface to a vapor–solid interface, causes the sudden rising of the wall temperature, leading to a melt down of the wall or to burn-out.

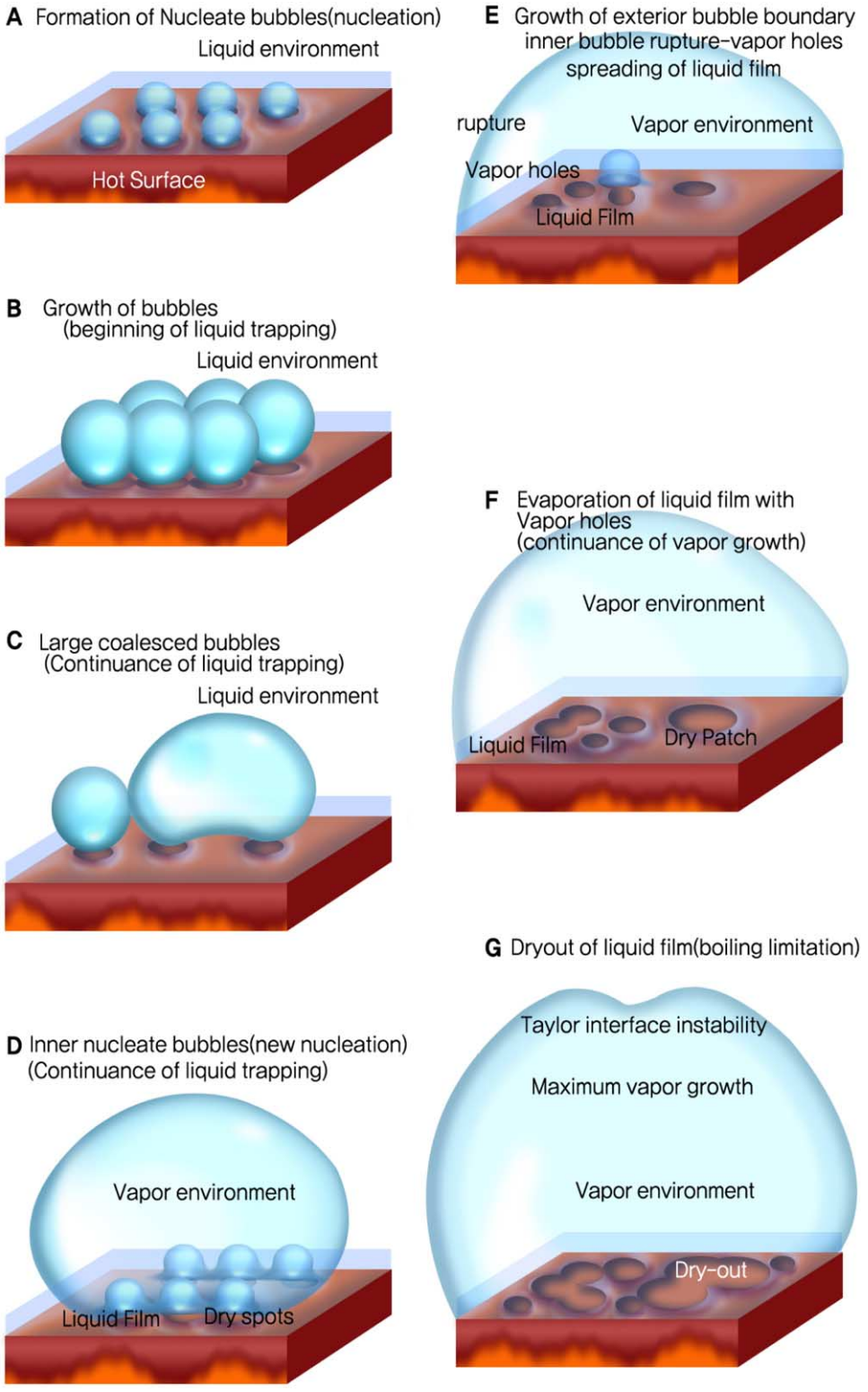

Fig. 11. A visual model for the formation and dryout of a liquid film under its vapor environment. The images are color-coded, with reddish brown and blue denoting hot surface and liquid film on a surface or the liquid film (outline) of a bubble, respectively.

3.3. Image model for life and death of a liquid film under a vapor environment

Based on the present observations, we have made a model for the formation and dryout of a liquid film under its vapor environment as shown in Fig. 11.

(A) The nucleation is initiated on a hot surface submerged in liquid. (B) Growth of bubbles proceeds until the departure condition of bubbles from the surface is achieved. At this time, liquid start to be trapped in interleaved space between growing bubbles and surface. (C) Coalescence of bubbles has a large vapor bubble form. Thus, liquid trapping continues between coalesced bubble and surface. (D) At this stage, such a coalescence of bubbles result in a vapor environment on a surface. Simultaneously nucleate bubbles continue to occur in interleaved liquid on a surface. (E) Bubbles inside a vapor environment make spontaneous breakup or rupture. Thus vapor holes are formed. Disturbed liquid at such a process spreads stably on a surface. (F) More liquid in the film evaporates into the vapor environment. (G) When all of liquid film has evaporated, the surface must be overheated due to poor heat transfer capability of the vapor environment.

4. Conclusions

We have reported here on the existence of a liquid film under a vapor environment which had been a theoretical premise of a principle mechanism of critical heat flux, significantly difficult to verify through experimental observations.

(a) Here, we show that a liquid film under a massive vapor bubble adheres to a heated solid surface.
(b) The liquid film comes into being trapped in a dynamic coalescence environment of nucleate bubbles, which grow and depart continuously from the heated surface.
(c) In its dryout process, the liquid film displays vapor "holes" originating from the rupture of discrete nucleating bubbles.
(d) The dryout process of the liquid film can be understood from the vaporization of rims of the holes and of smooth film region.

The experimental observations of this study will contribute to the ability of heat transfer community to provide actual depictions of the liquid film and the structure which are greatly important in principle mechanism of critical heat flux. This, in turn, will lead to a variety of practical applications for devices, such as micro- and macro-heat exchangers, MEMS heat transport devices, and actuators, as well as to a design for the enhancement of heat transfer or critical heat flux through understanding the principle mechanism.

Acknowledgements

We thank Prof. H.C. NO and Dr. D.W. Lee from KAIST, and Dr. S.Y. Chun, Dr. S.K. Moon, and Dr. S.H. Kim from KAERI for helpful discussions. This research was supported by Korea Atomic Energy Research Institute and Korea Ministry of Science and Technology.

Appendix

Terminology: *Vapor bubble*—discrete bubble, single bubble, nucleating bubbles from nucleation sites. *Microlayer*—annular wetting area under a discrete bubble. *Dry spot*—a round dry base under single discrete bubble. *Massive vapour bubble*—large bubble, large coalesced bubble, vapour clot due to coalescences of many bubbles. *Thin liquid film*—macrolayer, liquid sublayer under massive vapour bubble. *Vapor stems*—cross-section of dry spots in liquid sublayer under massive vapour bubble. *Dry patch*—large dry area due to coalescence of dry-spots or coalescence of bubbles in liquid film under a massive vapour bubble. *Hot spots*—dry spots with a locally higher temperature due to some reasons. *Vapor holes*—round dry area in liquid film or dry spots, vapour stems.

References

[1] Y. Hsu, R.W. Graham, Transport Processes in Boiling and Two-Phase Systems, American Nuclear Society, 1986.
[2] Z. Zhao, S. Glod, D. Poulikakos, Pressure and power generation during explosive vaporization on a thin-film microheater, Int. J. Heat Mass Transfer 43 (2000) 281–296.
[3] P. Sadasivan, P.R. Chappidi, C. Unal, R.A. Nelson, Possible mechanisms of macrolayer formation, Pool and External Flow Boiling, ASME (1992) 135–141.
[4] Y. Katto, S. Yokoya, Principal mechanism of boiling crisis in pool boiling, Int. J. Heat Mass Transfer 11 (1968) 993–1002.
[5] R.F. Gaertner, J.W. Westwater, Population of active sites in nucleate boiling heat transfer, Chem. Eng. Prog. Symp. 56 (1960) 39–48.
[6] D.B. Kirby, J.W. Westwater, Bubble and vapor behavior on a heated horizontal plate during pool boiling near burnout, Chem. Eng. Prog. Symp. 61 (1965) 238–248.
[7] C.L. Yu, R.B. Messler, A study of nucleate boiling near the peak heat flux through measurement of transient surface temperature, Int. J. Heat Mass Transfer 20 (1977) 827–840.
[8] S.H. Chang, I.C. Bang, W.P. Baek, A photographic study on the near-wall bubble behavior in subcooled flow boiling, Int. J. Thermal Sci. 41 (2002) 609–618.

[9] I.C. Bang, S.H. Chang, W.P. Baek, Visualization of the subcooled flow boiling of R-134a in a vertical rectangular channel with an electrically heated wall, Int. J. Heat Mass Transfer 47 (2004) 4349–4363.
[10] S.J. Ha, H.C. No, A dry-spot model of critical heat flux in pool and forced convection boiling, Int. J. Heat Mass Transfer 41 (2) (1998) 303–311.
[11] H.J. Chung, H.C. No, Simultaneous visualization of dry spots and bubbles for pool boiling of R-113 on a horizontal heater, Int. J. Heat Mass Transfer 46 (2003) 2239–2251.
[12] S. Lee, U.S. Choi, S. Li, J.A. Eastman, Measuring thermal conductivity of fluids containing oxide nanoparticles, ASME J. Heat Transfer 121 (1999) 280–289.
[13] I.C. Bang, S.H. Chang, Boiling heat transfer performance and phenomena of Al_2O_3–water nano-fluids from a plain surface in a pool, Int. J. Heat Mass Transfer 48 (2005) 2407–2419.
[14] J.G. Coller, J.R. Thome, Convective Boiling and Condensation, third ed., Clarendon press, Oxford, 1994.
[15] R. Yerushalmi-Rozen, T. Kerle, J. Klein, Alternative dewetting pathways of thin liquid films, Science 285 (1999) 1254–1256.
[16] Y. Haramura, Y. Katto, A new hydrodynamic model of critical heat flux, applicable widely to both pool and forced convection boiling on submerged bodies in saturated liquids, Int. J. Heat Mass Transfer 26 (1983) 389–399.
[17] A.E. Bergles, What is the real mechanism of CHF in pool boiling? Pool Ext. Flow Boiling, ASME (1992) 165–175.
[18] C.T. Avedisian, B. Osborne, F.D. McLeod, C. Curley, Measuring bubble nucleation temperature on the surface of a rapidly heated thermal ink jet heater immersed in a pool of water, Proc. R. Soc. Lond. A 455 (1999) 3875–3899.